

Using of the Mosaic-skeleton Method for Numerical Solution of Three-Dimensional Scalar Diffraction Problems

Sergei Smagin, Aleksei Kashirin, and Mariia Taltykina

Computing Center of FEB RAS, Khabarovsk, Russia
smagin@as.khb.ru, elomer@mail.ru, taltykina@yandex.ru
<http://www.ccfbras.ru/en/general>

Abstract. In the paper three-dimensional stationary scalar diffraction problems are considered. They are formulated in the form of boundary weakly singular Fredholm integral equations of the first kind with a single function, each of which is equivalent to the original problem. These equations are approximated by systems of linear algebraic equations, which are then solved numerically by an iterative method. In order to reduce the computational complexity, the mosaic-skeleton method is used at the stage of numerical solution of the systems.

Keywords: diffraction problem, Helmholtz equation, integral equation, mosaic-skeleton method, GMRES

1 Introduction

Three-dimensional stationary diffraction problems of acoustic waves are widely used in science and technology. Most often such problems are solved numerically, since their analytical solutions can be constructed only in simplest cases. The method of numerical solution of the initial problems should take into consideration that the solutions are found in unbounded domains, must satisfy the radiation condition at infinity, and are rapidly oscillating functions at large wave numbers. Keeping these limitations in mind, it is preferable to use methods of the potential theory for creating the algorithms for numerical solution. In this case, the three-dimensional problem in an unbounded domain can be reduced to a two-dimensional problem formulated on a closed surface of inclusion.

Using the methods of potential theory, two equivalent weakly singular boundary Fredholm integral equations of the first kind with one unknown function (density) [1–3] are constructed for the problem of diffraction. A special method of averaging kernels of weakly singular integral operators [4, 5] is used to build their discrete analogs. In this case, the unknown density is sought as a linear combination of continuously differentiable finite functions forming a partition of unity on the surface of inclusion. In the process of discretization of the integral equation, the surface integrals are approximated by expressions containing integrals over space \mathbb{R}^3 , which are then calculated analytically. This allows calculation of

coefficients of systems of linear algebraic equations (SLAE), approximating corresponding integral equations, by very simple formulas. Once the approximate solution of integral equation is found, the required approximate solution of the diffraction problem by using integral representations is restored in any point of space.

Matrices of the obtained SLAE are dense. The complexity of solving such SLAE by direct methods is $O(n^3)$, where n is the order of the system. It was established earlier [1] that the use of the generalized minimal residual method (GMRES) [6] allows to lower the complexity to $O(mn^2)$, where m is the number of iterations, which is much less than n and barely depends on it. The most time-consuming part of the algorithm of GMRES is the use of multiple matrix-vector multiplication. The time expenses on multiplication can be lowered using the "quick" method, the complexity of which is $o(n^2)$, when $n \rightarrow \infty$. The mosaic-skeleton method [7] – [11] can be used for already developed software for solving problems of mathematical physics. Its basic idea is to approximate the large blocks of dense matrices by low-rank matrices. As a result, the SLAE matrix is not fully computed and stored, but its approximation is used in the procedure of matrix-vector multiplication. In this case, the complexity of multiplication of this approximation by a vector is almost linear.

To implement the method in an already established program for numerical solution of diffraction problems, it is only necessary to add the procedure of creating and storing the approximate matrix and to change the module of matrix-vector multiplication, whereas the method of sampling and the calculation procedure of the elements of the original matrix remain the same. An additional advantage of this method is that, due to the cost effective storage of the approximate matrix, the requirements for computer resources are reduced.

The present work outlines the numerical method for solving three-dimensional problems of diffraction formulated as boundary Fredholm integral equations of the first kind and describes the use of the mosaic-skeleton method for the numerical solution of such problems. It also presents the results of numerical experiments, which allow us to judge the effectiveness of the approach.

2 The initial problem and its equivalent integral equations

Let us consider a three-dimensional Euclidean space \mathbb{R}^3 with orthogonal coordinate system $ox_1x_2x_3$, filled with a homogeneous isotropic medium with density ρ_e , with speed of propagation of acoustic oscillations c_e and absorption coefficient γ_e , which has a homogeneous isotropic inclusion, limited by the arbitrary closed surface Γ , with density ρ_i , speed of sound c_i and absorption coefficient γ_i . Let's denote domains \mathbb{R}^3 , occupied by the inclusion and containing medium, by Ω_i and Ω_e ($\Omega_e = \mathbb{R}^3 \setminus \bar{\Omega}_i$).

Suppose there are harmonic sound sources in space Ω_e , stimulating initial pressure wave field u_0 in the containing medium. Sound waves come through space and scatter, reaching the inclusion. As a result, there appear reflected

waves in domain Ω_e , and transmitted waves in domain Ω_i . Therefore, the complex amplitude of the complete field of pressures u can be presented as:

$$u = \begin{cases} u_i, & x \in \Omega_i, \\ u_e + u_0, & x \in \Omega_e, \end{cases}$$

where u_i , u_e are complex amplitudes of the pressure field of transmitted and reflected wave fields.

The inclusion, initial, reflected and transmitted pressure wave fields are shown in the Figure 1.

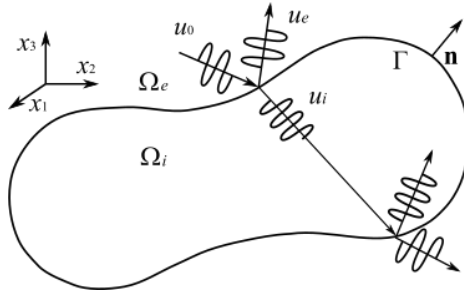


Fig. 1. Wave propagation in the inclusion and in the containing medium

Let's formulate the initial problem.

Problem 1. In bounded domain Ω_i of three-dimensional Euclidean space \mathbb{R}^3 and unbounded domain $\Omega_e = \mathbb{R}^3 \setminus \bar{\Omega}_i$, separated by closed surface $\Gamma \in C^{r+\beta}$, $r+\beta > 1$, find complex-valued functions $u_{i(e)} \in H^1(\Omega_{i(e)}, \Delta)$, which satisfy integral identities

$$\int_{\Omega_{i(e)}} \nabla u_{i(e)} \nabla v_{i(e)}^* dx - k_{i(e)}^2 \int_{\Omega_{i(e)}} u_{i(e)} v_{i(e)}^* dx = 0 \quad \forall v_{i(e)} \in H_0^1(\Omega_{i(e)}), \quad (1)$$

conjugation conditions on the material interface between Ω_i and Ω_e

$$\langle u_i^- - u_e^+, \mu \rangle_\Gamma = \langle f_0, \mu \rangle_\Gamma \quad \forall \mu \in H^{-1/2}(\Gamma), \quad (2)$$

$$\langle \eta, p_i N^- u_i - p_e N^+ u_e \rangle_\Gamma = \langle \eta, p_e f_1 \rangle_\Gamma \quad \forall \eta \in H^{1/2}(\Gamma),$$

as well as the radiation condition at infinity

$$\partial u_e / \partial |x| - ik_e u_e = o(|x|^{-1}), \quad |x| \rightarrow \infty, \quad (3)$$

if functions $f_0 \in H^{1/2}(\Gamma)$ and $f_1 \in H^{-1/2}(\Gamma)$ are set on the boundary Γ .

Here v^* is a complex conjugate function to v , $\langle \cdot, \cdot \rangle_\Gamma$ is duality ratio on $H^{1/2}(\Gamma) \times H^{-1/2}(\Gamma)$, which generalizes the inner product in $H^0(\Gamma)$, $u^\pm \equiv \gamma^\pm u$, $\gamma^- : H^1(\Omega_i) \rightarrow H^{1/2}(\Gamma)$, $\gamma^+ : H^1(\Omega_e) \rightarrow H^{1/2}(\Gamma)$ are trace operators, $N^- : H^1(\Omega_i, \Delta) \rightarrow H^{-1/2}(\Gamma)$, $N^+ : H^1(\Omega_e, \Delta) \rightarrow H^{-1/2}(\Gamma)$ are operators of normal derivatives [12], $f_0 = u_0^+$, $f_1 = N^+ u_0$,

$$k_{i(e)}^2 = \omega (\omega + i\gamma_{i(e)}) / c_{i(e)}^2, \quad \text{Im}(k_{i(e)}) \geq 0, \quad p_{i(e)} = c_{i(e)}^2 k_{i(e)}^{-2} \rho_{i(e)}^{-1},$$

ω is a wave circular frequency, $c_{i(e)} > 0$, $\rho_{i(e)} > 0$, $\gamma_{i(e)} \geq 0$. The definitions of functional spaces used hereinafter are available in [12].

Remark 1. If $\text{Im}(k_e) = 0$, then $u_e \in H_{\text{loc}}^1(\Omega_e, \Delta)$.

In works [1], [2] the next theorem was proven.

Theorem 1. *Problem 1 has no more than one solution.*

Let's introduce the following notation

$$(A_{i(e)}q)(x) \equiv \langle G_{i(e)}(x, \cdot), q \rangle_\Gamma, \quad (B_{i(e)}q)(x) \equiv \langle N_x G_{i(e)}(x, \cdot), q \rangle_\Gamma, \quad (4)$$

$$(B_{i(e)}^*q)(x) \equiv \langle N(\cdot)G_{i(e)}(x, \cdot), q \rangle_\Gamma, \quad G_{i(e)}(x, y) = \exp(ik_{i(e)}|x - y|) / (4\pi|x - y|).$$

The solution to problem 1 will be sought in the form of potentials

$$u_e(x) = (A_e q)(x), \quad x \in \Omega_e, \quad (5)$$

$$u_i(x) = (p_{ei}A_i(N^+u_e + f_1) - B_i^*(u_e^+ + f_0))(x), \quad x \in \Omega_i,$$

where $q \in H^{-1/2}(\Gamma)$ is an unknown density, $f_0 \in H^{1/2}(\Gamma)$, $f_1 \in H^{-1/2}(\Gamma)$, $p_{ei} = p_e/p_i$.

The kernels of these integral operators are fundamental solutions of the Helmholtz equations and their normal derivatives. Therefore, as shown in [2], they satisfy identities (1) and radiation condition at infinity (3). In addition, the fulfillment of the first of the matching conditions for them (2) automatically entails the fulfillment of the second matching condition. Substituting potentials (5) in the first matching condition, we obtain a weakly singular Fredholm integral equation of the first kind for defining unknown density q :

$$\langle Cq, \mu \rangle_\Gamma = \langle f_2, \mu \rangle_\Gamma \quad \forall \mu \in H^{-1/2}(\Gamma), \quad (6)$$

where

$$C = (0.5 + B_i^*)A_e + p_{ei}A_i(0.5 - B_e), \quad f_2 = -(0.5 + B_i^*)f_0 + p_{ei}A_i f_1.$$

Problem 1 allows another equivalent formulation in the form of Fredholm integral equation of the first kind with a weak singularity in the kernel [1]. We shall seek its solution in the form

$$u_i(x) = (A_i q)(x), \quad x \in \Omega_i, \quad (7)$$

$$u_e(x) = (A_e(f_1 - p_{ie}N^-u_i) - B_e^*(f_0 - u_i^-))(x), \quad x \in \Omega_e,$$

where $q \in H^{-1/2}(\Gamma)$ is an unknown density, $f_0 \in H^{1/2}(\Gamma)$, $f_1 \in H^{-1/2}(\Gamma)$, $p_{ie} = p_i/p_e$.

In this case problem 1 is reduced to equation

$$\langle Dq, \mu \rangle_\Gamma = \langle f_0, \mu \rangle_\Gamma \quad \forall \mu \in H^{-1/2}(\Gamma), \tag{8}$$

$$D = (0.5 - B_e^*)A_i + p_{ie}A_e(0.5 + B_i).$$

The next theorem is proved [1].

Theorem 2. Let $f_0 \in H^{1/2}(\Gamma)$, $f_1 \in H^{-1/2}(\Gamma)$, $\gamma_e > 0$ or ω is not the eigen frequency of the problem

$$\Delta u + k_e^2 u = 0, \quad x \in \Omega_i, \quad u^- = 0.$$

Then equations (6) and (8) are correctly solvable in the class of densities $q \in H^{-1/2}(\Gamma)$ and formulae (5) and (7) provide the solution to problem 1.

Remark 2. In cases where we are more interested in the wave field in domain Ω_e , it is preferable to use equation (6), which allows the calculation of the reflected field by a simpler formulae. For a similar reason, if we are interested in the transmitted wave field in domain Ω_i , it is preferable to use equation (8).

3 Numerical method

The applied method of numerical solution is presented in work [3] and appears to be the development of the technics proposed and tested for the first time in [4]. Let us briefly describe the general scheme of its implementation. Let us construct a surface Γ coating by system $\{\Gamma_m\}_{m=1}^M$ of neighborhoods of nodes $x'_m \in \Gamma$, lying within the spheres of radii h_m centered at x'_m , and denote its subordinate partition of unity by $\{\varphi_m\}$. In place of φ_m let us take functions

$$\varphi_m(x) = \varphi'_m(x) \left(\sum_{k=1}^M \varphi'_k(x) \right)^{-1}, \quad \varphi'_m(x) = \begin{cases} (1 - r_m^2/h_m^2)^3, & r_m < h_m, \\ 0, & r_m \geq h_m, \end{cases}$$

where $x \in \Gamma$, $r_m = |x - x'_m|$, $\varphi_m \in C^1(\Gamma)$ when $\Gamma \in C^{r+\beta}$, $r + \beta > 1$.

Approximate solutions of equations (6) and (8) will be sought on grid $\{x_m\}$,

$$x_m = \frac{1}{\bar{\varphi}_m} \int_\Gamma x \varphi_m d\Gamma, \quad \bar{\varphi}_m = \int_\Gamma \varphi_m d\Gamma,$$

the nodes are the centers of gravity of functions φ_m . We assume that for all $m = 1, 2, \dots, M$ inequalities are satisfied

$$0 < h' \leq |x_m - x_n|, \quad m \neq n, \quad n = 1, 2, \dots, M,$$

$$h' \leq h_m \leq h, \quad h/h' \leq q_0 < \infty,$$

where h, h' are positive numbers depending on M , q_0 does not depend on M .

Instead of unknown function q set on Γ we shall seek generalized function $q\delta_\Gamma$, acting according to the rule

$$(q\delta_\Gamma, \eta)_{\mathbb{R}^3} = \langle q, \eta \rangle_\Gamma \quad \forall \eta \in H^1(\mathbb{R}^3).$$

We shall approximate this function by expression

$$q(x) \delta_\Gamma(x) \approx \sum_{n=1}^M q_n \bar{\varphi}_n \psi_n(x),$$

where q_n are unknown coefficients,

$$\psi_n(x) = (\pi\sigma_n^2)^{-3/2} \exp(-(x - x_n)^2/\sigma_n^2), \quad \sigma_n^2 = 0.5\bar{\varphi}_n.$$

In paper [3] it is shown that for any functions $\eta \in H^1(\mathbb{R}^3)$ and $q \in H^1(\Gamma)$ equality

$$\langle q, \eta \rangle_\Gamma = \sum_{n=1}^M q_n \bar{\varphi}_n (\psi_n, \eta)_{\mathbb{R}^3} + O(h^2).$$

Approximation of the density of a single layer potential by a volume density allows us to obtain simple formulae for approximating integral operator $A_{i(e)}$ from (4). The theoretical justification of the presented approach is given in [4].

The integral operators from (4) on Γ are approximated by expressions [1, 5].

$$\langle A_{i(e)}q, \varphi_m \rangle_\Gamma \approx \sum_{n=1}^M A_{i(e)}^{mn} q_n, \quad m = 1, 2, \dots, M, \quad (9)$$

$$A_{i(e)}^{mn} \equiv A_{mn}(k_{i(e)}),$$

$$A_{mn}(k) = \frac{\bar{\varphi}_m \bar{\varphi}_n}{8\pi r_{mn}} \exp(\mu_{mn}^2 - \gamma_{mn}^2) (w(z_{mn}^-) - w(z_{mn}^+)), \quad n \neq m,$$

$$A_{mm}(k) = \frac{\bar{\varphi}_m^2}{4\pi} \exp(\mu_{mm}^2) \left(ikw(\mu_{mm}) + \frac{\sqrt{2\pi}}{\bar{\varphi}_m} \left(\frac{\bar{\varphi}_m}{\pi\sigma_m} + 2\sigma_m - \frac{k^2\sigma_m^3}{3} \right) \right),$$

$$\sigma_{mn}^2 = \sigma_m^2 + \sigma_n^2, \quad \mu_{mn} = 0.5k\sigma_{mn}, \quad z_{mn}^\pm = \mu_{mn} \pm i\gamma_{mn},$$

$$\gamma_{mn} = r_{mn}/\sigma_{mn}, \quad i^2 = -1,$$

$$w(z) = -\frac{2i}{\sqrt{\pi}} \exp(-z^2) \int_z^\infty \exp(t^2) dt,$$

$$\langle aq + B_{i(e)}q, \varphi_m \rangle_\Gamma \approx \sum_{n=1}^M B_{i(e)}^{mn} q_n, \quad m = 1, 2, \dots, M, \quad a = \pm 0.5, \quad (10)$$

$$\langle aq + B_{i(e)}^* q, \varphi_m \rangle_\Gamma \approx \sum_{n=1}^M B_{i(e)}^{nm} q_n, \quad m = 1, 2, \dots, M, \quad (11)$$

$$B_{i(e)}^{mn} = \frac{\eta_{mn}}{4\pi r_{mn}^2} \exp(ik_{i(e)} r_{mn}) (ik_{i(e)} r_{mn} - 1) \bar{\varphi}_m \bar{\varphi}_n, \quad n \neq m,$$

$$B_{i(e)}^{mm} = (-|a| + a + Gs_m) \bar{\varphi}_m, \quad \eta_{mn} = \sum_{l=1}^3 n_{ml} \frac{x_{ml} - x_{nl}}{r_{mn}}, \quad Gs_m = - \sum_{n \neq m}^M \frac{\eta_{nm} \bar{\varphi}_n}{4\pi r_{mn}^2},$$

n_{ml} are components of the unit vector of the external normal to the surface at point x_m .

The operators on the left sides of equations (6) and (8) are approximated by the composition of operators (9)–(11):

$$\langle Cq, \varphi_m \rangle_\Gamma \approx \sum_{n=1}^M C_{ie}^{nm} q_n, \quad \langle Dq, \varphi_m \rangle_\Gamma \approx - \sum_{n=1}^M C_{ei}^{nm} q_n, \quad m = 1, 2, \dots, M, \quad (12)$$

$$C_{ie}^{nm} = B_i^{nm} A_e^{mn} - p_{ei} A_i^{mn} B_e^{mn},$$

and the right sides of equations (6) and (8) by formulae

$$\langle f_2, \varphi_m \rangle_\Gamma \approx \sum_{n=1}^M (p_{ei} A_i^{mn} f_{1n} - B_i^{nm} f_{0n}), \quad \langle f_0, \varphi_m \rangle_\Gamma = \bar{\varphi}_m f_{0m}, \quad (13)$$

$$f_{lm} = \langle f_l, \varphi_m / \bar{\varphi}_m \rangle_\Gamma, \quad l = 0, 1, \quad m = 1, 2, \dots, M.$$

Solving the corresponding SLAE, we find the approximate values of the density of integral equations at discretization points. After that, an approximate solution of the diffraction problem using integral representations can be calculated at any point in space.

4 Mosaic-skeleton method

Let us introduce the definitions necessary for describing the mosaic-skeleton method [7]. Let A_k be block matrix $A^{n \times m}$, and $\Pi(A_k)$ be matrix of size $n \times m$, resulting from A_k by adding zeros up to A .

Definition 1. *The systems of blocks $\{A_k\}$ will be called covering A , if*

$$A = \sum_k \Pi(A_k),$$

and mosaic partitioning A , if, in addition, $\bigcap_k A_k = \emptyset$.

Definition 2. *The mosaic rank of matrix $A \in \mathbb{C}^{n \times m}$, corresponding to some covering, is number*

$$\text{mr } A = \sum_k \text{mem } A_k / (n + m), \quad (14)$$

where the sum is taken over all blocks of covering $A_k \in \mathbb{C}^{n_k \times m_k}$, and $\text{mem } A_k = \min\{n_k m_k, (n_k + m_k) \text{rank } A_k\}$.

The mosaic rank determines the memory requirements for storing the mosaic partitioning of matrix A , and also the computational complexity of matrix-vector multiplication.

An important indicator of the effectiveness of this method is the compression factor I [7]. It is defined by the following formulae

$$I = \frac{\text{mem } A_p}{\text{mem } A} 100, \tag{15}$$

where $\text{mem } A_p$ is the amount of memory required to store a matrix in a low-rank format, $\text{mem } A$ is the amount of memory for storing the original matrix.

Definition 3. *We shall call a matrix of uv^* kind a skeleton, where u and v are column vectors, v^* denotes the row-vector Hermite-conjugate to vector v .*

From definition 3 it follows that $\text{rank}(uv^*) = 1$.

The mosaic-skeleton method consists of three phases: constructing a cluster tree, creating a list of blocks and finding a low-rank approximation. For the first phase, the input data is a grid, on which discretization is carried out. The set of all points of the grid is called a zero-level cluster (or a root of the tree). At each step, the original cluster is split into several disjoint subclusters. This continues until the level of the tree reaches the prescribed one. As a zero-level cluster, we can take a cube, and plunge the domain on the border of which the grid is built there. When moving to the next level of the tree, each edge of this cluster bisects, resulting in 8 subcubes. Then, all the points belonging to the original cube are distributed across 8 subcubes, forming 8 subclusters (some of them might be empty). On reaching the maximum level of k , the number of clusters equals 8^k .

The next step is creating the list of blocks. Any two clusters determine a block in a matrix. If the points of the clusters are geometrically separated from each other, the block enters a far zone and an approximation will be constructed for it, or, otherwise, it enters a near zone, and the elements of the blocks will be calculated by formulae (12).

At the final stage, the blocks of the far zone are approximated by low-rank matrices. Such matrices can be sought in different ways [10, 11]. In paper [13] the cross of the matrix row and column is chosen as a template. A current approximation is built on the cross at each step. This algorithm is called incomplete cross approximation [8, 14].

Algorithm 1. Incomplete cross approximation.

Approximation of matrix A of size $n \times m$ by matrix $A^{(r)}$, being the sum of r skeletons.

1. Let p be the number of the calculated skeleton. At this step, we assume that $p = 1$ and select an arbitrary number j_p from the column of matrix A .
2. In the column with number j_p we calculate all the elements of matrix A , then, subtract the elements of all previously obtained skeletons in these positions from them. In the obtained column u_p we find the maximum element in modulus. Let it be located in the row with number i_p .

3. We calculate the row of matrix A with number i_p and subtract from it the elements of all already found skeletons in their respective positions. In the obtained row v_p^* we find the maximum element in modulus. It should be noted that an element from the column with number j_p cannot be selected again. The number of the column in which the maximum element is found will be denoted by j_{p+1} .
4. Along the cross with centre (i_p, j_p) we build a skeleton so that the coefficients of matrix

$$A^{(p)} = \sum_{\alpha=1}^p \frac{u_\alpha v_\alpha^*}{A_{i_\alpha j_\alpha}} \quad (16)$$

coincide with the coefficients of the original matrix in positions p of computed columns j_1, \dots, j_p and p of calculated rows i_1, \dots, i_p .

5. We check the stopping criterion. If it is satisfied, the calculation stops. If it is not satisfied, we set $p := p + 1$ and repeat the algorithm from step 2.

An approximation (16) is considered to be sufficiently accurate if inequality (stopping criterion)

$$\|A - A^{(p)}\|_F \leq \varepsilon \|A^{(p)}\|_F,$$

where ε is a relative approximation error, $\|\cdot\|_F$ is a Frobenius norm [15], is satisfied.

To verify this criterion, it is necessary to calculate nm of the elements of matrix A , which is very time-consuming. The number of operations can be reduced by using the upper estimate of $\|A - A^{(p)}\|_F$, obtained in [8]

$$\|A - A^{(p)}\|_F \leq (l - p) \|u_p v_p^*\|_F / |A_{i_p j_p}| = (l - p) \|u_p\|_F \|v_p\|_F / |A_{i_p j_p}|,$$

where $l = \min(n, m)$.

Here the stopping criterion takes the form of

$$(l - p) \|u_p\|_F \|v_p\|_F / |A_{i_p j_p}| \leq \varepsilon \|A^{(p)}\|_F. \quad (17)$$

Using recurrence formulae we can obtain next result

$$\|A^{(p)}\|_F^2 = \|A^{(p-1)}\|_F^2 + 2\operatorname{Re} \left(\sum_{\alpha=1}^{p-1} \frac{(u_p^* u_\alpha)(v_\alpha^* v_p)}{A_{i_\alpha j_\alpha} A_{i_p j_p}^*} \right) + \frac{\|u_p\|_F^2 \|v_p\|_F^2}{|A_{i_p j_p}|^2},$$

$$\|A^{(1)}\|_F = \frac{\|u_1\|_F \|v_1\|_F}{|A_{i_1 j_1}|}, \quad p \geq 2.$$

5 Numerical results

The program for the numerical solution of diffraction problems is written in Fortran 90 and has the form of a console application, designed to run on multiprocessor computing systems. Intel Fortran Compiler performs as a compiler,

Intel Math Kernel Library (Intel MKL) and implementation of the OpenMP standard for the compiler are also used. The above mentioned software is used in the computing cluster of CC FEB RAS (<http://hpc.febras.net/>). The cluster consists of one subcontrol and thirteen compute nodes. The compute node with four Six Core AMD Opteron™ 8431 processors, with clock frequency of 2.40 GHz and 96 GB of RAM has been involved in testing. To read more information about the program, see [16].

Example 1. The diffraction problem of a plane acoustic wave on a triaxial ellipsoid with semi-axes (0.75, 1, 0.5) centered at the origin of coordinates and having three different sets of parameters of the host medium and inclusion. The complex amplitude of the initial wave field of pressures has the form $u_0(x) = \exp(ik_e x_3)$, $f_0 = u_0^+$, $f_1 = N^+ u_0$, parameters of the media: *I*) $k_i = 8, \rho_i = 3, k_e = 5.5, \rho_e = 1$; *II*) $k_i = 15.5, \rho_i = 5, k_e = 9, \rho_e = 4$; *III*) $k_i = 21, \rho_i = 7, k_e = 30.5, \rho_e = 9.5$.

In all the examples, the diffraction problem was solved twice: using the mosaic-skeleton method in GMRES and without it. In the process discretization of equations (6) and (8) was carried out by formulas (12) and (13), the order of matrix M ranged from 1032 to 64139. Hereinafter the accuracy of GMRES amounted to 10^{-7} , and the accuracy of the low-rank approximations was 10^{-5} . The level of the cluster tree varied from 4 to 5. Further, squares denote the first set of media parameters, circles stand for the second set and triangles mark the third set in all the graphs.

In this case, the solutions found approximately were compared with the solutions found on a denser grid, i.e. with 64139 sampling points. This is because the analytical solution of Example 1 is unknown. The relative errors of solution of the problem in Example 1 using equation (6) and (8) are shown in Figures 2. The solid lines indicate errors u_i , and the dashed lines represent errors u_e . According to the numerical experiments, the method has the second order of accuracy, as the errors fall twofold when the order of matrix is doubled ($O(M^{-1}) = O(h^2)$). The errors were calculated in the norm of grid functions $H_h^0(\Omega_{i(e)})$.

The time spent on the solution of SLAE depending on the order of matrix M with the mosaic-skeleton method and without it is shown in Figures 3 for equation (6). The results for equation (8) are similar. Hereinafter, the time t is presented in seconds. The dashed lines show the time for solving SLAE using the mosaic-skeleton method, and the solid lines indicate the time for solving SLAE without it. When using the mosaic-skeleton method in GMRES, the solution time is 115 times less (at $M = 64139$ for the third set of parameters for equation (6)) than without the fast method. When the number of nodes is doubled, the time for solving SLAE using the mosaic-skeleton method increases 2.5 times on average.

Tables 1 and 2 show the values of the mosaic rank and compression factor for SLAE, approximating the integral equation (6), depending on the number of grid points. For equation (8) almost the same results were obtained. This is because the kernels of equations (6) and (8) have similar properties as they are

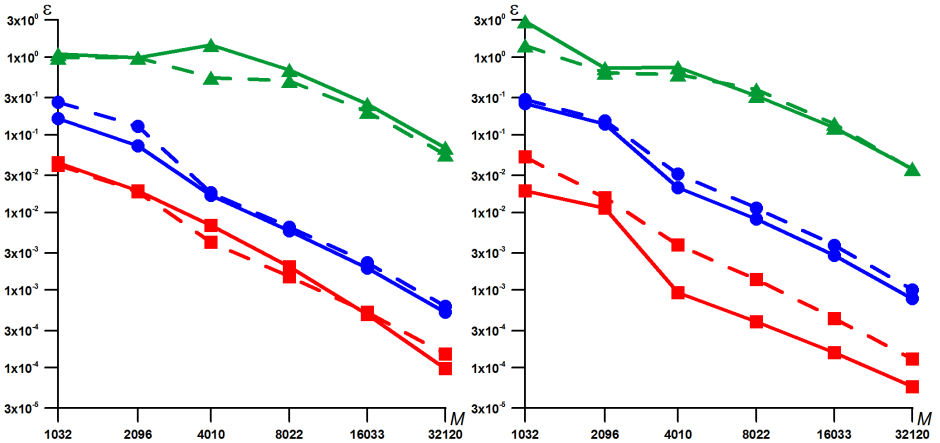


Fig. 2. Errors of solutions u_i (solid lines) and u_e (dashed lines) for the problem in Example 1, obtained with the help of equations (6) and (8), respectively

compositions of similar integral operators. The mosaic rank was calculated using formula (14), and the compression factor by formula (15). The numerical experiments show that the mosaic rank increases like $O(\ln^3(M))$, and the compression factor, from a certain M , decreases like $O(\ln^3(M)/M)$.

Table 1. Mosaic ranks for the problem in Example 1.

$k \setminus M$	1032	2096	4010	8022	16033	32120	64139
I	493.1	751.9	991.0	1244.1	1517.1	1845.1	2241.0
II	509.9	818.5	1103.0	1376.8	1666.3	2004.4	2410.3
III	518.0	948.5	1327.9	1677.7	2011.6	2380.7	2810.7

Table 2. Compression factors for the problem in Example 1.

$k \setminus M$	1032	2096	4010	8022	16033	32120	64139
I	95.6	71.7	49.4	31.0	18.9	11.5	7.0
II	98.8	78.1	55.0	34.3	20.8	12.5	7.5
III	100.0	90.5	66.2	41.8	25.1	14.8	8.8

Example 2. The problem of diffraction on a triaxial ellipsoid with semi-axes (0.75, 1, 0.5) centered at the origin is considered. The incident field is generated by a point source

$$u_0(x) = \exp(ik|x - x_0|)/|x - x_0|,$$

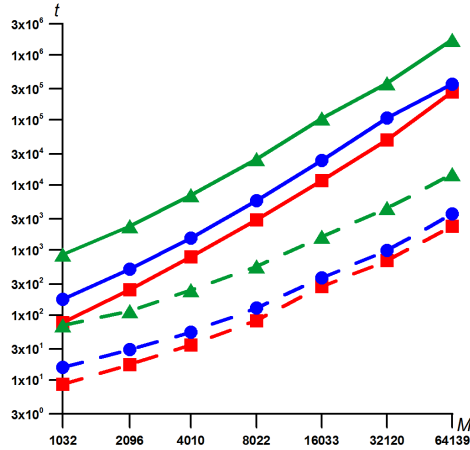


Fig. 3. SLAE solution time for the problem with the mosaic-skeleton method (dashed lines) and without it (solid lines) for equation (6) in Example 1

where $x_0 = (1.125, 1, 0.75)$. The sets of parameters of the containing medium and inclusion are the same as in Example 1.

The relative errors of solutions $u_{i(e)}$ for the problem in Example 2 formulated in the form of equation (6) and (8) are shown in Figures 4. The solid lines indicate errors u_i , and the dashed lines represent errors u_e . All the errors are calculated in the norm of grid functions $H_h^0(\Omega_{i(e)})$. When we increase the order of the matrices twofold, they also halve, as in the above example.

The values of mosaic rank and compression factor for the problem in Example 2 formulated in the form of equation (6) are shown in Tables 3 and 4, respectively. The mosaic rank, just as in the previous example, grows at the rate of $O(\ln^3(M))$, and the compression factor falls like $O(\ln^3(M)/M)$. Almost the same results were obtained for equation (8).

Table 3. Mosaic ranks for the problem in Example 2

$k \setminus M$	1032	2096	4010	8022	16033	32120	64139
I	493.1	751.9	991.0	1244.1	1517.1	1845.1	2241.0
II	509.9	818.5	1103.0	1376.8	1666.3	2004.4	2410.3
III	518.0	948.5	1327.9	1677.7	2011.6	2380.7	2810.7

Figures 5 show the real and imaginary parts of solution u_e for the first set of media parameters in Example 2 on the interval $-5 \leq x_1 \leq 5, x_2 = 0, x_3 = 1$ and on the interval $x_1 = 0, -5 \leq x_2 \leq 5, x_3 = 1$, respectively. It is evident that solution u_e oscillates rapidly and slowly decreases while distancing from the inclusion.

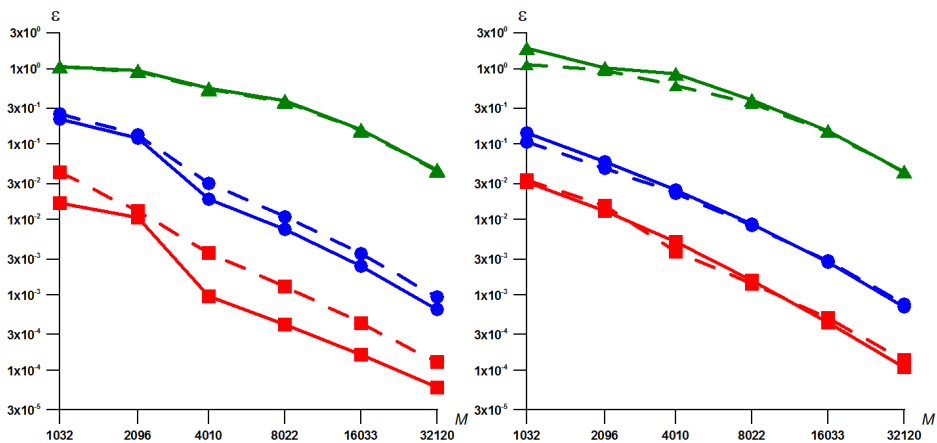


Fig. 4. Errors of solutions u_i (solid lines) and u_e (dashed lines) for the problem in Example 2, obtained with the help of equations (6) and (8), respectively

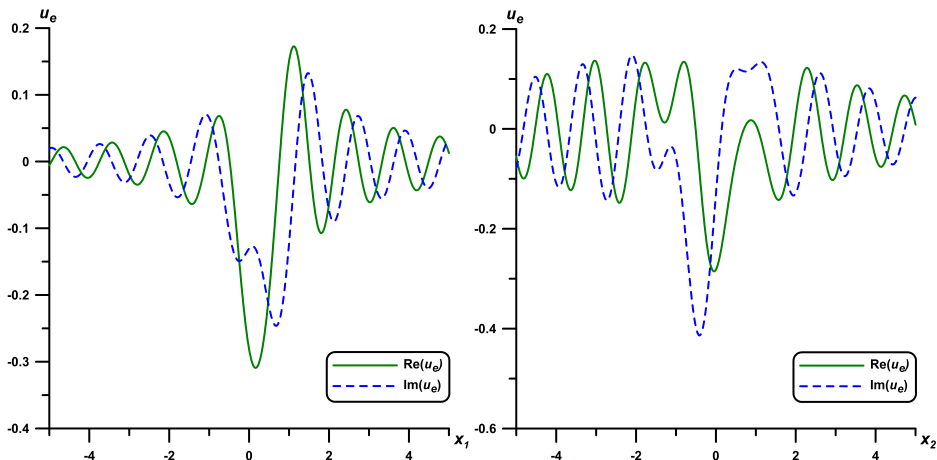


Fig. 5. Real and imaginary parts of solution u_e in Example 2

Table 4. Compression factors for the problem in Example 2

$k \backslash M$	1032	2096	4010	8022	16033	32120	64139
I	95.6	71.7	49.4	31.0	18.9	11.5	7.0
II	98.8	78.1	55.0	34.3	20.8	12.5	7.5
III	100.0	90.5	66.2	41.8	25.1	14.8	8.8

6 Conclusion

We have studied the possibilities of using the mosaic-skeleton method for numerical solution of three-dimensional diffraction problems of acoustic waves, for which two new formulations have been offered in the form of boundary Fredholm integral equations of the first kind with one unknown function. The method has been implemented on the stage of solving linear systems. All of the most labor-intensive computing processes have been parallelized using OpenMP. The obvious advantage of this approach compared to the others, for example, to a fast multipole method, is that the mosaic-skeleton method can be used in already existing software for the numerical solution of integral equations of diffraction theory. Thereat only the algorithms for calculating the coefficients of linear systems and matrix-vector multiplication are changed. Using the multipole method and other similar methods involves creating virtually new computing algorithms and programs.

Numerical experiments have shown that the modification of numerical algorithms for solving diffraction problems with the mosaic-skeleton method leads to a significant acceleration of their work while maintaining the same accuracy of calculations.

References

1. Kashirin, A.A.: Research and Numerical Solution of Integral Equations of Three-dimensional Stationary Problems of Diffraction of Acoustic Waves. PhD thesis, Khabarovsk (2006) (in Russian)
2. Kashirin, A.A., Smagin, S.I.: Generalized Solutions of the Integral Equations of a Scalar Diffraction Problem. *Diff. Equat.* 42(1), 79–90 (2006)
3. Kashirin, A.A., Smagin, S.I.: Numerical Solution of Integral Equations of a Scalar Diffraction Problem. *Dokl. Akad. Nauk*, 458(2), 141–144 (2014)
4. Smagin, S.I.: Numerical Solution of an Integral Equation of the First Kind with a Weak Singularity for the Density of a Simple Layer Potential. *Comp. Math. Math. Phys.*, 28(11), 1663–1673 (1988)
5. Kashirin, A.A., Smagin, S.I.: Potential-based Numerical Solution of Dirichlet Problems for the Helmholtz Equation. *Comp. Math. Math. Phys.* 52(8), 1492–1505 (2012)
6. Saad, Y., Schultz, M.: GMRES: a Generalized Minimal Residual Algorithm for Solving Nonsymmetric Linear Systems. *SIAM Journal on Scientific and Statistical Computing.* 7(3), 856–869 (1986)
7. Tyrtshnikov, E.E.: Methods for Fast Multiplication and Solution of Equations. *Matrix Methods and Computations*, INM RAS, Moscow. 4–41 (1999) (in Russian)

8. Savostyanov, D.V.: Polilinear Approximation of Matrices and Integral Equations. PhD thesis, Moscow (2006) (in Russian)
9. Goreinov, S.A.: Mosaic-skeleton Approximations of Matrices Generated by Asymptotically Smooth and Oscillatory Kernels. Matrix Methods and Computations, INM RAS, Moscow. 41–76 (1999) (in Russian)
10. Tyrtyshnikov, E.E.: Mosaic-skeleton Approximations. *Calcolo*, 33(1), 47–57 (1996)
11. Tyrtyshnikov, E.E.: Incomplete Cross Approximations in the Mosaic-skeleton Method. *Computing*, 64(4), 367–380 (2000)
12. McLean, W.: Strongly Elliptic Systems and Boundary Integral Equations. Cambridge University Press, Cambridge (2000)
13. Bebendorf, M.: Approximation of Boundary Element Matrices. *Numer. Math.* 86(4), 565–589 (2000)
14. Kashirin, A.A., Smagin, S.I., Taltykina, M.Y.: Mosaic-Skeleton Method as Applied to the Numerical Solution of Three-Dimensional Dirichlet Problems for the Helmholtz Equation in Integral Form. *Computational Mathematics and Mathematical Physics*, 4(56), 612–625 (2016)
15. Meyer, C.D.: Matrix analysis and applied linear algebra. SIAM, Philadelphia (2000)
16. Kashirin, A.A., Smagin, S.I., Taltykina, M.Y.: Realization of Mosaic-skeleton Method in Dirichlet problems. *Informatics and control systems*, 4(46), 32–42 (2015)